Oxide film characteristics of AZ91 magnesium alloy in casting conditions

A. R. Mirak[1], M. Divandari*[1], S. M. A. Boutorabi[1] and J. Campbell[2]

Molten magnesium alloys oxidise rapidly during casting and handling if adequate prevention measures are not taken. New oxide films that form in a very short time during pouring seem to be one of the main reasons for dross-like defects. The characteristics of these new oxide films were observed. The magnesium alloy AZ91 was selected for the study. Samples were prepared based on the technique in which an oxide–metal–oxide sandwich was made by bubble impingement. After impingement the contact areas of two adjacent and entrapped bubbles were selected for the study. Features such as thickness, size, morphology and chemical composition of the oxide film have been examined and shown by SEM. Possible consequences of the morphology of the oxide film were discussed.

Keywords: Oxide films, Mg alloys AZ91, Folded double films, Oxide–metal–oxide sandwich

Introduction

Molten magnesium metal oxidises rapidly in air, leading to complete burning of the melt surface in the crucible if there is enough time and no precautionary measures are taken.[1–3] With such a great tendency to oxidise, Mg alloys are reported to be very sensitive to turbulence during pouring, leading to characteristic defects in the castings.[4]

As soon as the liquid Mg alloy is poured, the freshly created surface oxidises. The entrainment of the newly created oxide into the bulk of the molten alloy necessarily occurs by a kind of folding process in which a double film is created characterised by a dry surface to dry surface contact (Fig. 1).[4] The interfaces wetted by (i.e. in atomic contact with) the melt are on the outside of the folded double film. The inner, unwetted surfaces of the doubled film are folded face to face, representing an unbonded interface in the liquid and therefore effectively constitute a crack when molten metal is solidified (Fig. 2).[4–6] Such a description of events in the melting and handling processes involved in casting is becoming generally accepted. However, oxide films play a major role in the formation of casting defects as has been discussed by different researchers.[7–11] Such effects seem to be especially critical in the casting of Mg alloys.

Most of research on the oxidation of molten metal has been carried out on stagnant melts.[12–18] Characterisation of the surface films formed on molten magnesium in different protective atmospheres has been carried out and presented by some workers.[11,12] However, in the casting process, the molten metal is in motion rather than stagnant. Thus, the oxide film layer is continuously subjected to deformation forces. Since the oxide film is expected to have little or no plasticity, it will tear when subjected to tension, but on exposure to the atmosphere, the freshly revealed magnesium will quickly reoxidise.[19]

So far, little research has been carried out on the nature of magnesium oxide films in the flowing (nonstagnent) state. The experiment in this work is based on a technique (oxide–metal–oxide sandwich formation) that has been introduced by one of authors. The technique seems to have good potential for the investigation of film formation characteristics, in very short times, in different alloys. Figure 3 shows oxide films formed in short time in two aluminium alloys taken from the inside of a trapped bubble in the casting. The scales of the two images are very close so that one can clearly compare the size and the morphology of the oxide film in both cases.[20,21]

Experimental

The chemical composition of the AZ91 alloy used in this work is Mg–8·7Al–0·5Mn–0·1Zn. Oxide–metal–oxide (OMO) sandwich samples were taken based on a technique explained elsewhere.[5] Following to the pouring of molten metal into a simple cylindrical shape casting via bottom gating system, trying to reduce the surface turbulence to the minimum possible level, a steady succession of bubbles was artificially introduced via a silica tube into the base of a casting. The inter and outer diameter of this tube was 1 and 2 mm respectively. If solidifying metal hinders the rise of a bubble, the subsequent bubble collides with it, generating a composite layer named here after OMO sandwich. The contacting region between the bubbles consists of a triple layer composed of the oxide films from each of the bubbles, and residual metal that happened to be trapped in between. By introducing enough bubbles plenty of the

[1]Iran University of Science and Technology, Narmak 16844, Tehran, Iran
[2]The University of Birmingham, B15 2TT, UK

*Correspondent author, email divandari@iust.ac.ir

Received 17 October 2006; accepted 19 October 2007
DOI 10.1179/136404607X256042

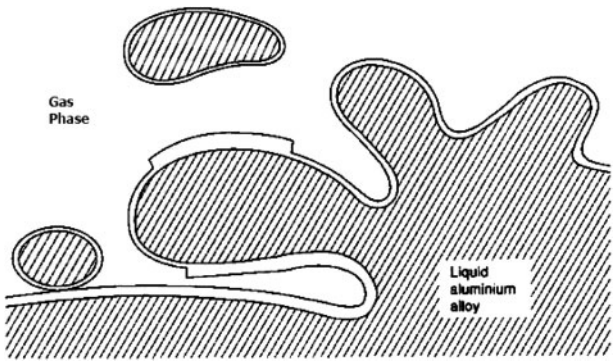

1 Schematic view of oxide film on surface of film forming alloys[4]

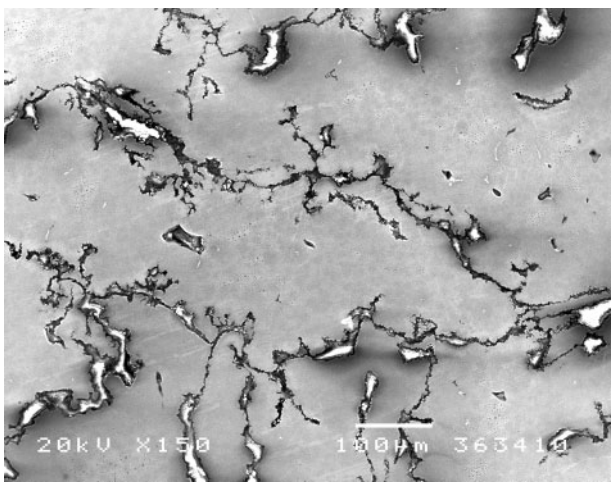

2 Tangled oxide films in Al–Mg alloy acting like crack[6]

OMO sandwich samples were made before allowing the casting to freeze. A schematic drawing of the technique and the sample studied in this work is shown in Fig. 4.

Silica sand containing 2% sulphur as an inhibitor and sodium silicate binder cured with carbon dioxide was used as the moulding material. For all experiments, the melt temperature was held at $650 \pm 5^{\circ}C$. Melting was carried out in an electrical furnace with SO_2 gas as cover for protecting molten metal from oxidation. For air bubbling into the casting compressed air was supplied at 0·3 MPa to a pressure gauge. An electrical valve was used to control the size and the number of bubbles. The oxide film morphology was studied using a scanning electron microscope (SEM). Energy dispersive X-ray (EDX) microanalysis was performed for detection of the composition of the oxide layers.

Table 1 Wrinkles size of oxide films measured in three different alloys

	Al–7Si–Mg		Al–5Mg		Mg alloy–AZ91			
Alloy	Min.	Max.	Min.	Max.	Min.	Max.*	Max.†	Max.‡
Thickness, µm	0·02	0·05	0·5	0·7	1	3	5	20

*Indicated in Fig. 5.
†indicated in Fig. 6.
‡Indicated in Fig. 7.

Results and discussion

Figure 5 shows typical oxide films of an AZ91 alloy draped on dendrites. The images were taken from the inside of a trapped bubble in the casting. They are indicative of the morphology of young oxide films of magnesium alloy formed in short time. They are similar to those found in other alloys, but possibly with significantly greater thickness.[20,21] The tips of dendrites are quite visible underneath the draped oxide film. The morphology and the size of folds in this alloy can be measured and compared with two alloys that are shown in Fig. 3 (Table 1).

It can be seen that the morphology of the oxide films in the images shown in Fig. 5 is quite rough in comparison with Al–7Si–Mg alloy shown in Fig. 3*a*. The rough and folded morphology of oxide films in Mg based alloys has been reported previously.[16,17] Individual folds of the films on the tips of dendrites (Fig. 5) are seen to be less than 5 µm, indicating a film thickness of less than 2·5 µm, which is thicker than what was previously reported in Al–5Mg and Al–7Si–Mg alloys shown in Fig. 3.[20,21]

Figure 6 shows images taken from the contact area between two adjacent bubbles (the OMO sandwich). Figure 6*a* shows a relatively uniform region of the oxidised surface, illustrating film that appears to be perhaps 2–5 µm thick, arranged in fine concertina-like

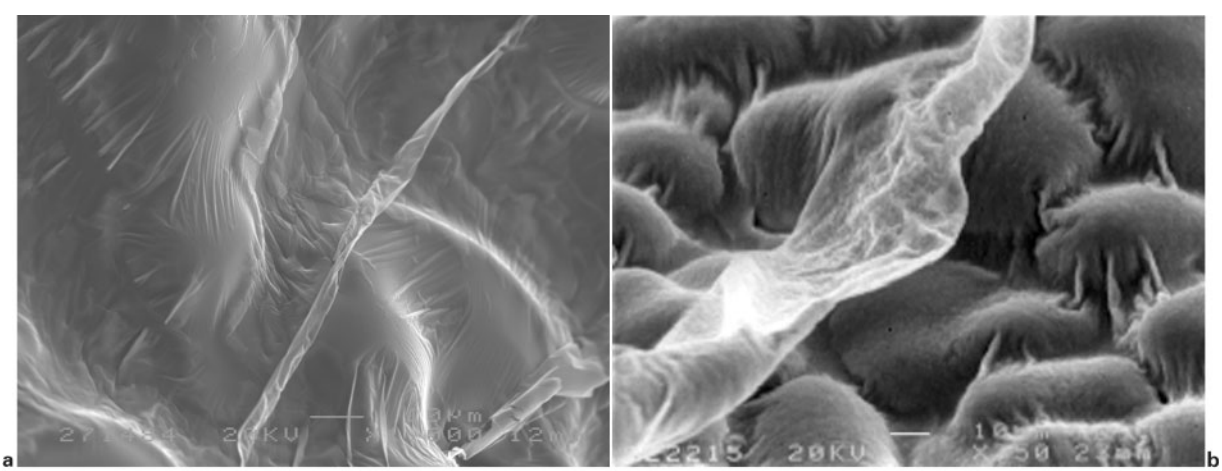

3 Images (SEM) taken from inside trapped bubble in *a* Al–7Si–Mg and *b* Al–5Mg: morphology of folded oxide films and size of their folds and wrinkles are distinguishable from underlying dendrite tips; note scale of two images which are very close together[20,21]

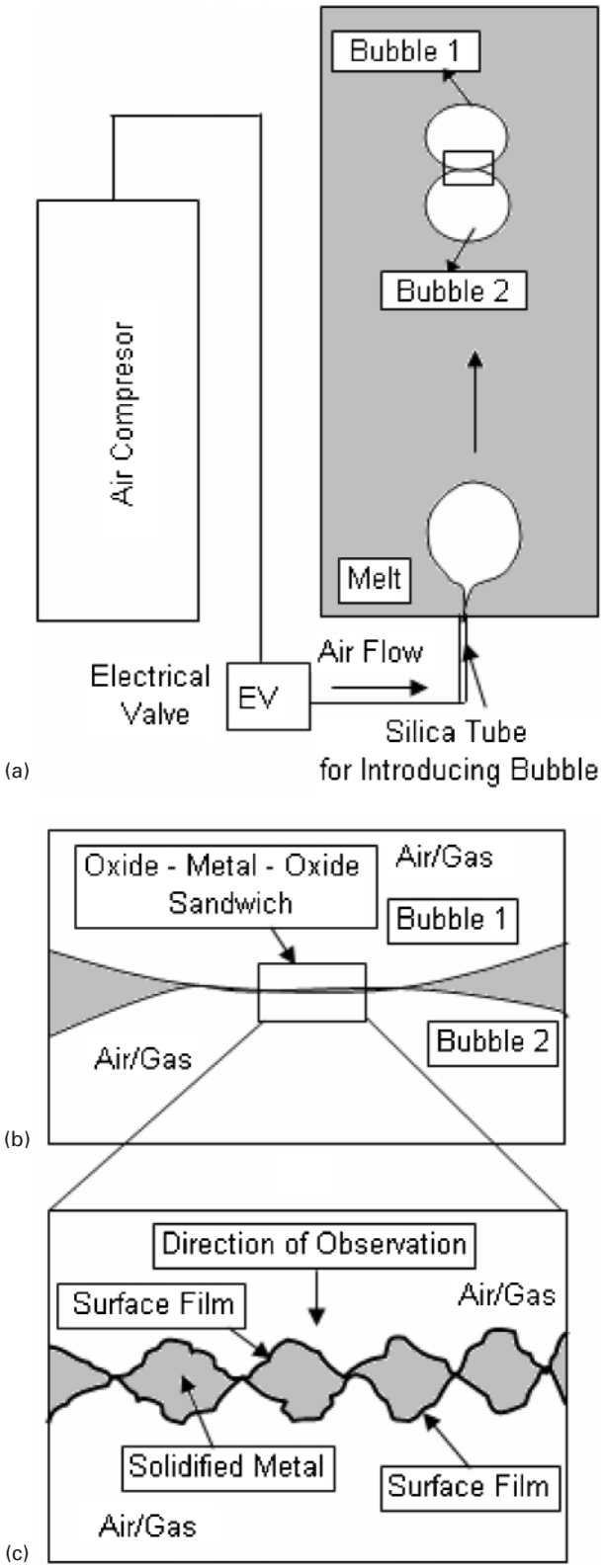

4 ***a*** **schematic drawing of setup of experiments for taking OMO sandwich samples and** ***b*** **close view of OMO sandwich and** ***c*** **more details of OMO sandwich showing direction of observation for taking SEM images**

folds of wavelength about 10 μm. Figure 6*b* illustrates another region of the same sample having relatively macroscopic folds of the order of 50 μm wavelength. It seems that oxide films in this figure have formed in the condition while there has been either more time for oxidation or more oxygen for the continuation of the oxidation process in comparison with the films shown in Fig. 5. It is also interesting to note that if one calculates the volume of air that can be encapsulated between folds of the films[22] in these two conditions, one can speculate that the possibility of porosity formation would be higher in the case shown in Fig. 6 in comparison with that shown in Fig. 5. Considering Fig. 1 it is clear that such thick films are likely to cause more damage to properties in Mg alloy castings compared to the problems caused by films in Al alloy castings. It is worth mentioning that while the tips of dendrites are visible in Figs. 3 and 5, they are not clear in Fig. 6, which seems to be the result of the thickness of film in the later case.

Figure 7 shows two images of thick oxide films that were typical of those seen in this study. The colour of such thick oxide films was mostly black when viewed with the unaided eye. It can be seen from the SEM image that the sizes of the folds are in the range of tens of microns. In addition, some fine crystals have started to form on the surface of the folds. Crystallisation on the surface of oxide films in Mg alloys, similar to that shown in the Fig. 7*b* has been reported by others.[21] A typical EDX analysis of the film is shown in Fig. 7*c*.

The remnant of a bubble trail is shown in Fig. 7*a*. Bubbles are known to rotate and spiral as they rise. Spiraling motion of the bubble will tighten the rope-like trail. It is reported that the film expand over the crown of the bubble while it rises and continuing to expand of this area causes the film to fold and crease.[4,6]

Figure 8 shows differences in the size and morphology of folds in AZ91 alloy all taken from a similar magnification. A comparison between the size of folds in Mg alloy and Al alloys (Al–7Si–Mg, Al–5Mg) is shown in Table 1. The formation of Mg oxide seems to exert a potent influence on the morphology of oxide films as seen in Fig. 3. Focusing now on the folded nature of the oxide films one can envisage the future use of physical and/or mathematical modelling techniques to estimate the amount of air and/or gas that might be entrapped between folds. Comparing Fig. 3, which shows two different Al alloys, and Figs. 5–7 in this work illustrate the varieties of size and morphology of folds.

One can see the dendrites formed in the OMO sandwich as shown in Fig. 9. In Fig. 9*a* a region with coarse folds on the left side of the image is noticeable. These folds appear to obscure the underlying dendrites. The small white region in the middle left of the image (the triangle-like shape denoted by the arrow) is the area where two nearly transparent layers of oxide films have come together without any metal trapped in between. A closer image of this region is shown in Fig. 9*b*. Fig. 4*c* shows the detailed sketch of the condition when two bubbles come close together. This is similar to that reported for aluminium alloys.[20,21] However, this work reveals a unique ability of the sandwich technique to provide thin samples of matrix alloy, sufficiently thin to appear transparent to electrons in the SEM. In this way inclusions inside the dendrites can be seen, indicating the potential of the technique for the study of particles that have nucleated the solid. Further work in this area is planned.

It is interesting to see the variety of the folds even in a small area from Fig. 9. Such a variation has not been noticed in the Al–7Si–Mg,[20] but one could see a similar

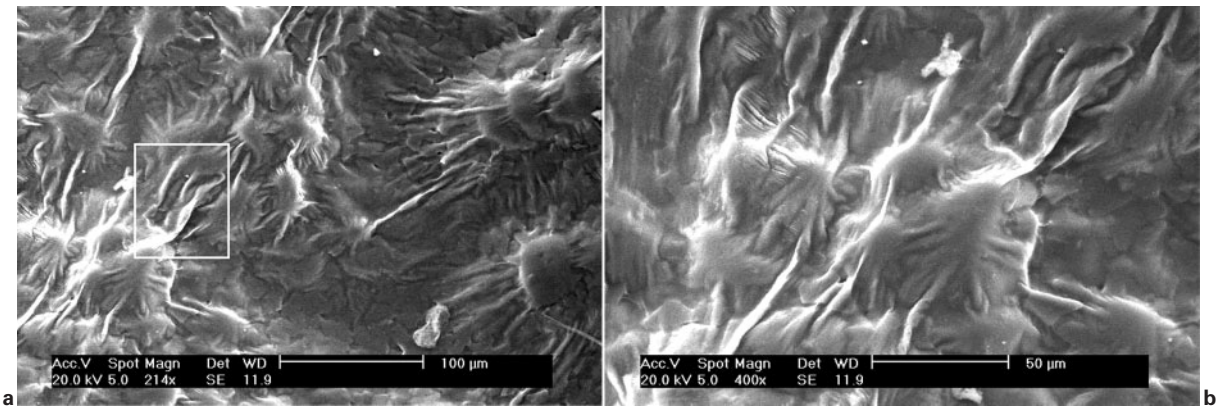

a b

5 Folded oxide film draped over dendrites inside trapped bubbles, *a* note morphology and size of wrinkles on tips of dendrites; *b* shows close view of left bottom part of same image

phenomenon in Al–5Mg alloy as shown in Fig. 3.[21] This similarity is clearly associated with of the presence of Mg and its tendency toward rapid oxidation.

Difference between folds and wrinkles

Figure 10 shows the type of hugely folded surface oxide films in this work. These folds seem to be in the range of 50 µm which are nearly ten times bigger than what was seen in the Fig. 5. In fact two quite different types of folding were noticed in this research with some cases in between. The first types, which may be called wrinkles, are similar to what generally is visible in Figs. 5 and 6*a*. These wrinkles seem to be the result of the difference between contraction coefficient of the molten metal and its surface oxide film which is a ceramic phase. In other words these micro folds are the result of contraction stress exerted on the surface film as shown in Fig. 11. Noting that while the melt is solidifying and therefore naturally contracting to some extent the surface oxide film would not contract the same amount because of its different nature.

The second types of folding are similar to what is visible in the Fig. 10. These types of folds, which seem to be mechanically induced folds, are the result of turbulence of the molten metal while it has been filling the mould. Figure 1 clearly shows how this type of the fold may form knowing that stress component of the turbulence would have different effects on the surface oxide film and the melt underneath. One of the best micrographs that show both of theses folding phenomenon together is shown in Fig. 3*b*. The big fold in the middle part of the image is mechanically induced as a result of turbulence and the wrinkles seen in the figure are the result of contraction stress. Exactly similar case is shown in Fig. 3*a* noting that the surface film in Al–7Si–Mg alloy is quite thin in comparison with either Al–5Mg or Mg based alloys.

Looking now to the left side of the Fig. 6*b* one can notice the difference between the size and the morphology of the folds in this region and the rest of micrograph. These folds seem to be the result of simultaneous effect of both contraction stress and the mechanical stress which possibly have been exerted on the interface of the surface oxide film and the melt. Similar condition is probable for the films shown in Fig. 7. The only differences in these two cases are the characteristics of the surface of the film having noticed that in the latter there has been more time for MgO crystals to start growing.

Noticing the mentioned difference in the morphology of the surface oxide films, however, on being folded into the melt by turbulence during the pour, the accidental entrapment of air between films will be expected to lead to the continuation of oxidation, leading to the closure of the gap between the folded halves of the bifilm, and the impingement of the convoluted morphologies (Fig. 12). Such closed bifilms probably to have weak strength,[22] and probably represent a more serious defect

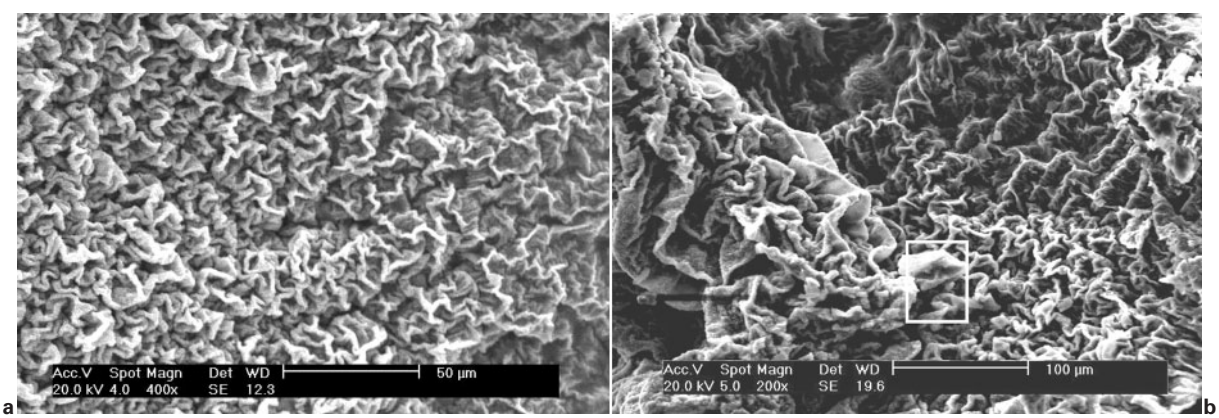

a b

a uniform folded oxide film in specimen; *b* this image shows another region from same specimen

6 Folded oxide film draped over dendrites in OMO sandwich: difference in the size and shape of folds and wrinkles are noticeable

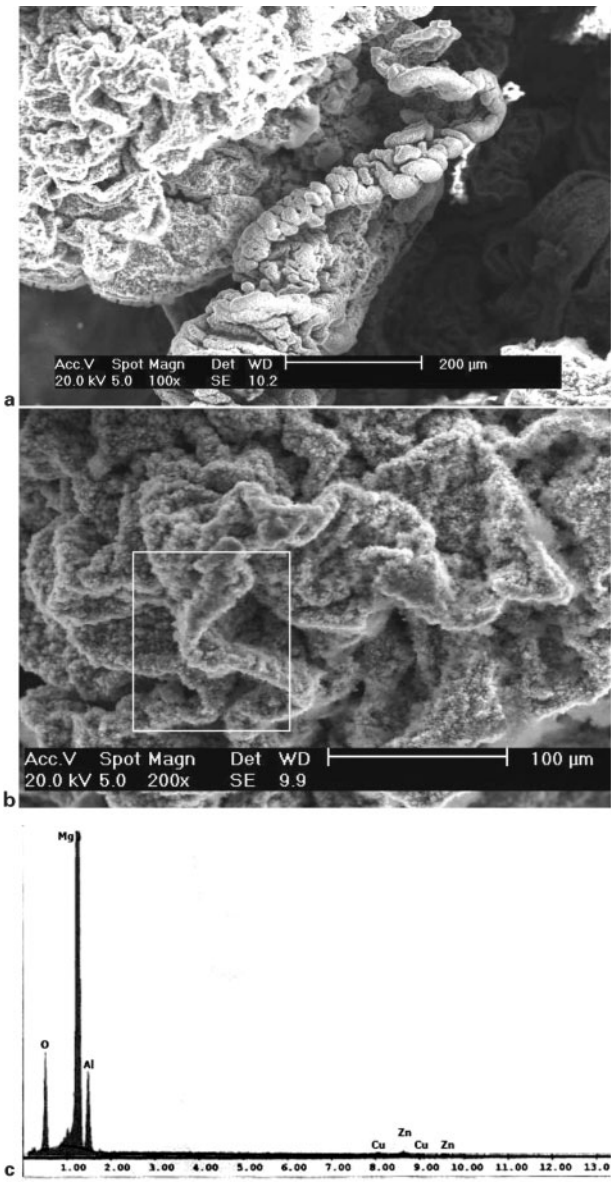

a spiral appearance of feature of bubble trail remnant; *b* on surface of film crystals of MgO have started to grow, appearing as fine scale granulation; *c* EDX analysis of oxide films shown in Fig. 7*b*

7 Oxide film that appears black when seen with unaided eye, when seen under SEM

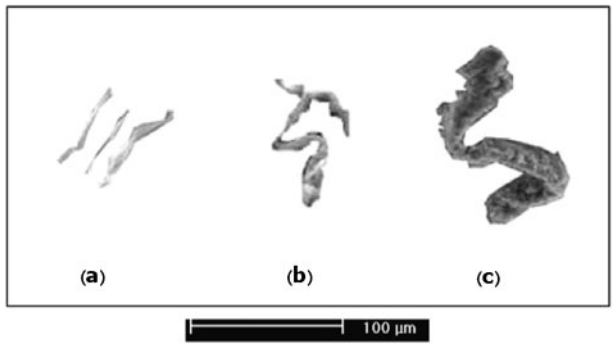

a sample from Fig. 5*a*; *b* from Fig. 6*b*; *c* from Fig. 7*b*

8 Examples of fragments of typical films taken from SEM images, illustrating differences in size and morphology of folds all taken from similar magnification

than a similar enfolded film in an aluminium alloy as already mentioned. A comparison between the roughness of surface film of Al–Mg alloy and that of Al–7Si–Mg alloy has been already reported.[20,21]

Conclusions

The following conclusions can be drawn from this work.

1. The contacting interface between impinged bubbles represents an elegant and powerful means for studying surface films of liquid metals.

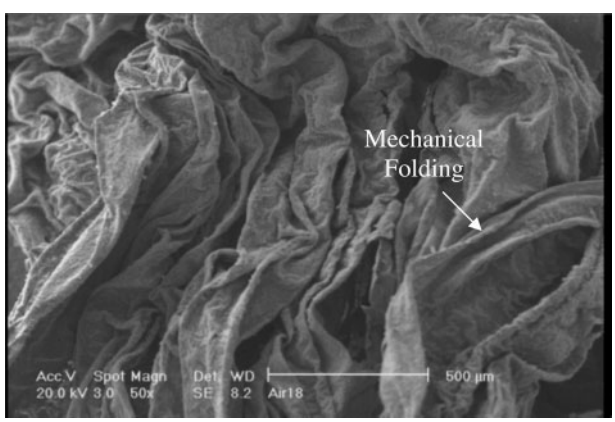

10 Image (SEM) taken from surface oxide films accompanying molten metal which have been subjected to deformation stresses as result of motion of melt

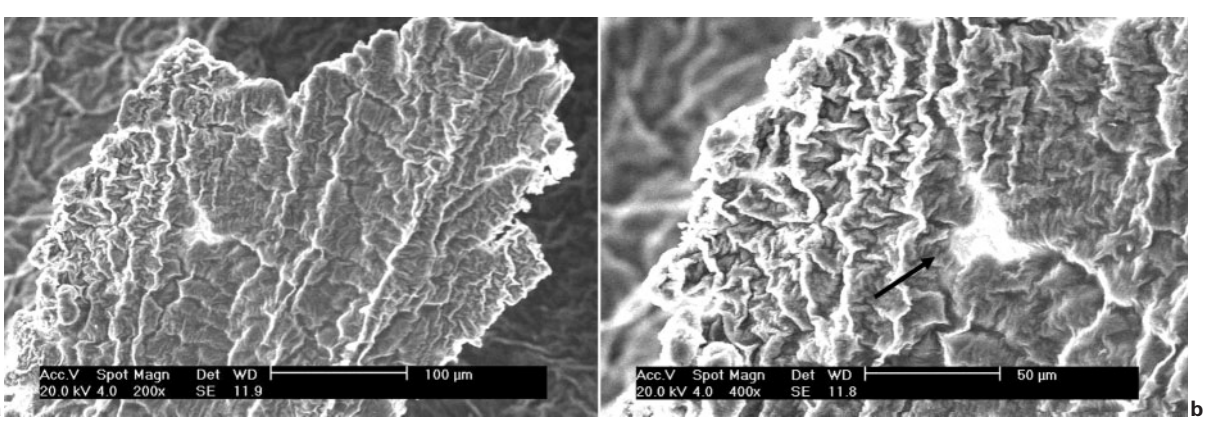

9 *a* oxide–metal–oxide sandwich of AZ91 alloy and *b* closer view of middle to left region of same image showing different morphology of oxide film on far right: white triangle area that is area where two layers of oxide film in sandwich have come to contact; there is no metal between two layers of film in this area

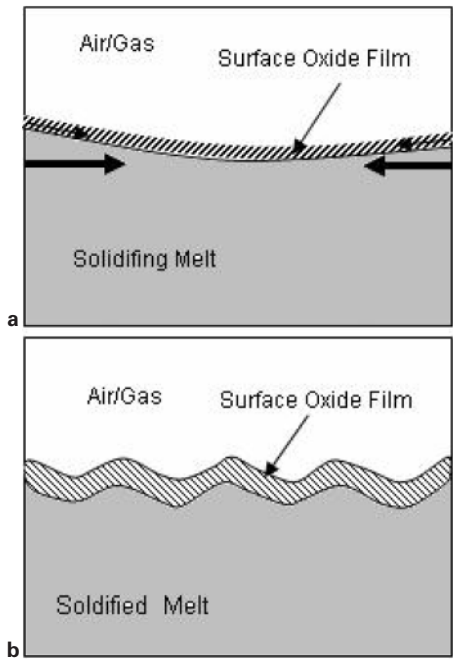

a before contraction; *b* after contraction

11 Drawing showing contraction stress while melt is solidifying

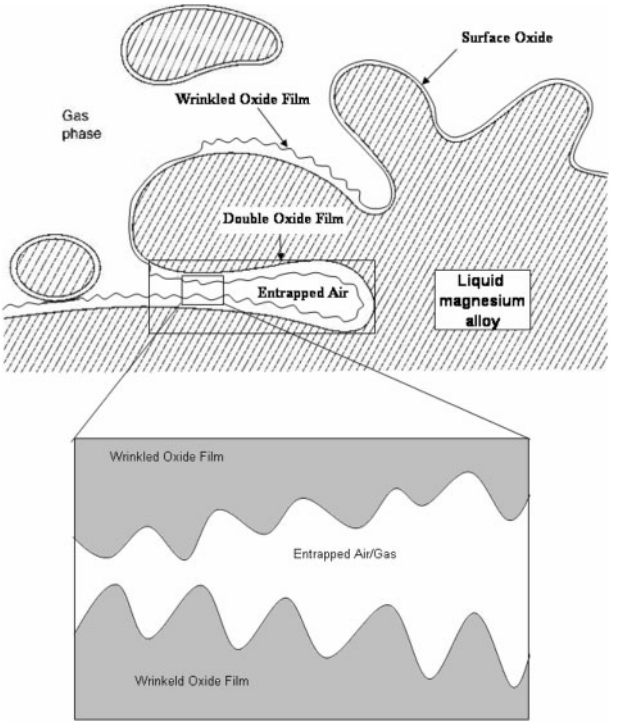

12 Schematic drawing of mechanism of folding of oxide film on surface of molten metal and entrapment mechanism of air/gas into folds

2. Two types of folds were visible in this research, the first type named wrinkles which forms as a result of contraction stress and the second type which are bigger and can be called folds are possibly the result of mechanical stress on the melt in turbulent motion.

3. The morphology of the oxide films is likely to be an indication of the amount of air that may be retained by the film, noting the fold morphology of the films.

4. The volume of the entrapped air might be a criterion for assessing the seriousness of the folded oxide film defects and their effectiveness as a crack and as an initiation site for the gas porosity.

References

1. S. C. Erickson, J. F. King and T. Mellerud: *Foundry Manag. Technol.*, 1998, **126**, (6), 38–45.
2. J. W. Fruehling and J. D. Hanawalt: *AFS Trans.*, 1969, **77**, 159–164.
3. E. F. Emley: 'Principles of magnesium technology'; 1966, Oxford, Pergamon Press.
4. J. Campbell: 'Casting'; 2003, Oxford, Butterworth-Heinemann.
5. M. Divandari and J. Campbell: *Aluminum Trans.*, 2000, **2**, 233–238.
6. M. Divandari and J. Campbell: *AFS Trans.*, 2001, 01–048, 1–10.
7. C. Nyahumwa, N. R. Green and J. Campbell: *AFS Trans.*, 1998, **58**, 215–223.
8. N. R. Green and J. Campbell: *AFS Trans.*, 1994, **102**, 341–347.
9. J. Runyoro, S. M. Boutorabi and J. Campbell: *AFS Trans.*, 1992, **100**, 225–234.
10. C. H. Caceres and B. I. Selling: *Mater. Sci. Eng. A*, 1996, **A220**, 109–116.
11. X. Dai, X. Yang, J. Campbell and J. Wood: *Mater. Sci. Technol.*, 2004, **20**, (4), 505–513.
12. J. L. Roberge and M. Richard: *Mater. Sci. Forum*, 1996, **3**, 135–140.
13. L. Rault, M. Allbert, M. Prin and A. Dubus: *Light Met.*, 1996, 345–355.
14. S. Impey, D. J. Stepheson and J. R. Nicholls: *J. Mater. Sci. Technol.*, 1988, 1126–1132.
15. G. Peterson, E. Overlid, G. Tranell, J. Fenstad and H. Gjestlad: *Mater. Sci. Eng. A*, 2002, **A332**, 285–294.
16. S. P. Cashion, N. J. Richetts and P. C. Hayes: *J. Light Met.*, 2002, **2**, 37–42.
17. S. P. Cashion, N. J. Ricketts and P. C. Hayes: *J. Light Met.*, 2002, **2**, 43–47.
18. X. Zeng, Q. Wang, Y. Lu, W. Ding, Y. Zhu, C. Zhai, C. Lu and X. Xu: *Mater. Sci. Eng. A*, 2001, **A301**, 154–161.
19. B. S. You, W. W. Park and L. S. Chung: *Scr. Mater.*, 2000, **42**, 1089–1094.
20. M. Divandari and J. Campbell: *Int. J. Cast Met. Res.*, 2004, **17**, (3), 182–187.
21. M. Divandari and J. Campbell: *Int. J. Cast Met. Res.*, 2005, **18**, (3), 187–192.
22. J. Campbell and P. Fox: *Scr. Mater.*, 2000, **43**, 881–886.